

Metrics of resolution and performance for CD-SEMs

David C Joy^{a,b}, Yeong-Uk Ko^a, and Justin J Hwu^a

^aEM Facility, University of Tennessee, Knoxville, TN 37996

^bOak Ridge National Laboratory, Oak Ridge, TN 37831

This program is now known as "ImageJ" or "FIJI". It's implemented in Java and runs on both Macs and Windows machines. It's freeware & can be downloaded from the web

ABSTRACT

The performance of scanning electron beam instruments such as CD-SEMs can be defined in terms of parameters such as the beam probe size, the spatial resolution, and the signal to noise ratio of the image. A knowledge of these quantities is important in verifying the fact that an instrument meets its specification, and subsequently for tracking and optimizing its performance during use. Analytical methods based on the power spectrum (2-D Fourier transform analysis) of images are now beginning to be used for these purposes but care must be exercised to ensure reliable and meaningful results. Two new methods are suggested which can offer more detailed information about the microscope performance while avoiding the pitfalls of the simpler technique. Code implementing these tests, written as a plug-in macro for the well known NIH Image program, is available on-line.

Keywords: scanning electron microscope, resolution, signal to noise, probe size, Fourier transform

1. INTRODUCTION

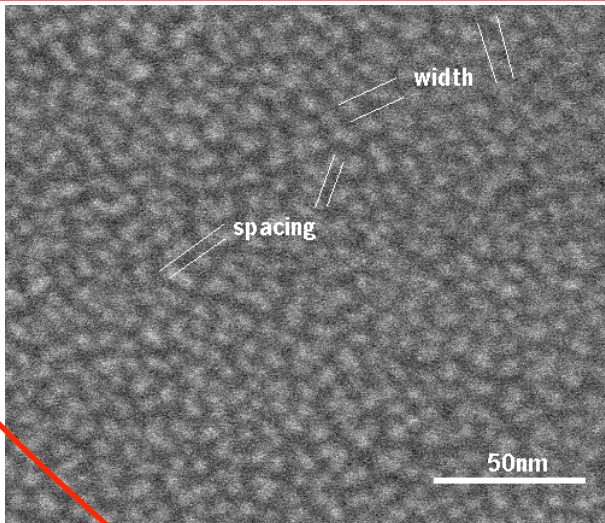
Scanning electron microscopes designed for the critical dimension metrology (CD-SEMs) must achieve a resolution approaching 1nm for the current technology nodes¹. Verifying that the tool is reaching the required level of performance when it is delivered, and subsequently monitoring its performance during use, requires that tests be available which can quantify the parameters such as probe size, resolution, the signal to noise ratio of the image under standard operating conditions etc., which define the performance level. In addition many electron beam tools are now used in a semi-automatic fashion with little or no operator supervision. There is thus a need for techniques which can monitor the performance of the tool to ensure that it remains within acceptable limits. Ideally such tests should be capable of being performed transparently during normal operation of the SEM, they should require no special specimen, and they should produce results that are unambiguous and demonstrably realistic. This paper describes some techniques designed to extract resolution and other information about the imaging process from micrographs.

2. BASIC TECHNIQUES

The common procedure for attempting to determine the resolution of a SEM has been to image a sample such as a gold or gold-palladium coating on a suitable substrate (figure 1) and to measure either the smallest objects that can be discerned, or the smallest spacing between objects that is visible in the micrograph. Such a procedure is subject to many objections. The result is highly dependent on the sample that is used, and the chosen sample is usually quite atypical of the types of objects that are normally to be

*Correspondence: Email: djoy@utk.edu; WWW: <http://web.utk.edu/~srcutk/>; Phone 865 974-3642; Fax 865 974 - 9449

This program is now known as "ImageJ" or FIJI.



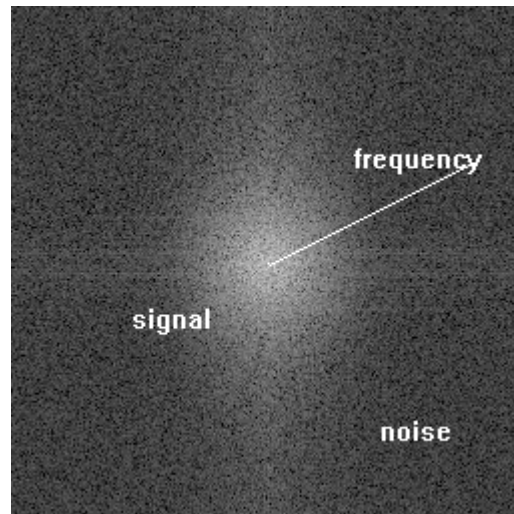
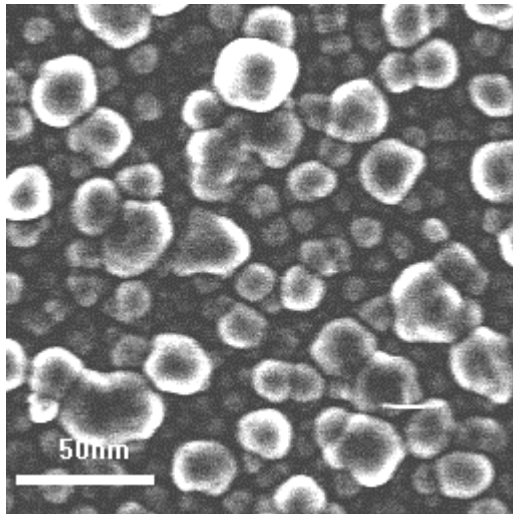
1. High resolution image of a gold-palladium layer on silicon illustrating the 'measurement' of resolution from feature size and spacing.

imaged and so resolutions determined in this way are not properly representative of the routine performance of the instrument. The measurement also only uses a very small fraction of all of the information in the micrograph and, finally, it assumes that the observer making the measurement can correctly distinguish, on a pixel by pixel basis, between genuine signal and random noise. Since high resolution images are of necessity of low signal to noise ratio this assumption is clearly suspect.

The basis of an objective and reliable method for the measurement of resolution is to obtain a diffractogram in the form of the power spectrum, i.e. the two-dimensional Fourier

transform, of the image². Figure 2 shows an image and the corresponding diffractogram power spectrum computed by a straightforward application of the fast Fourier transform (FFT)

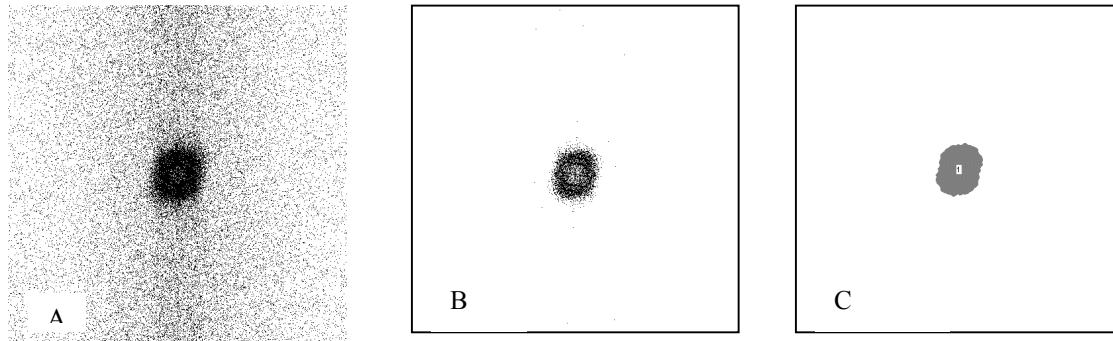
procedures in the NIH Image³ or SCION Image⁴ image processing programs. The intensity distribution of the different spatial frequencies in the image is displayed with the frequency increasing radially from the center of the transform. The signal intensity can be seen to decrease with increasing frequency until it eventually merges into the random noise background of the microscope. The spatial frequency at which this occurs is the highest frequency at which information is transferred through the microscope from the specimen to the display device, and it therefore the resolution limit of the SEM. The boundary separating signal from noise plots the variation of spatial resolution with directions in the image. In a correctly aligned microscope the spatial resolution will be the same in all directions, and so the signal intensity distribution should be circular. An elliptical intensity profile therefore indicates astigmatism in the beam probe and the ratio of the major to the minor axes of the ellipse is a measure of the stigmatic error.



2. Micrograph of oxide particles on a silicon substrate and (b) the corresponding diffractogram (two dimensional power spectrum) of the image. In the diffractogram the spatial frequency increases from the center of the image. The regions of signal information and noise are identified.

While it is readily possible to obtain the power spectrum from any image processing program capable of executing and displaying an FFT, obtaining quantitative data requires further processing capability. An

powerful commercial software and hardware package capable of recording SEM images and displaying their power spectrum and the resultant analysis in real time is available⁵. All of the examples in this paper were obtained using the NIH Image, or the Windows equivalent SCION Image, programs and a specially written 'macro' routine, called SMART (Scanning Microscope Analysis and Resolution Testing), which provides the required functions and computations. The SMART macro works identically for either NIH or SCION image and can be freely downloaded from the world wide web⁶.



3. Analysis of a diffractogram to determine image resolution. (a) The power spectrum generated from an ROI 512*512 pixels in size of the sample shown in figure 1. (b) The power spectrum after thresholding to remove noise, (c) the binary image for measurement by the stereology functions of NIH Image.

In order to measure the resolution from an image several steps are involved. First (figure 3a) the contrast of the power spectrum is enhanced by non-linear processing so that the signal and the noise contributions can be visualized more easily. Next (b) the user sets the image threshold control to define the boundary between the signal and the noise to an appropriate value. Too low a value leads to the inclusion of significant random noise, too high a value will exclude real signal information. The image is then converted to a binary image (c). The stereological functions provided within NIH or SCION Image can then automatically fit an ellipse to the binary signal distribution and report the length of the major and minor axes of the ellipse. If the length of the major axis is L_m (pixels), the width of the region of interest from which the transform was obtained is ROI (pixels), and if P is the number of pixels per micrometer in the original micrograph, then the resolution is given by the relation

$$resolution = \frac{1000 * ROI}{L_m * P} (nm) \quad (1)$$

and the stigmatic error is then $(L_m - L_n)/L_m$ where L_n is the minor axis of the fitted ellipse. On a typical PC the total computation time, excluding the time required for the operator to choose a threshold level, is one or two seconds for a 512*512 ROI.

3. PROBLEMS WITH FFT ANALYSIS

Although the Fourier based analysis procedure is a considerable step forward it must be applied with some care or else misleading or erroneous results will be produced.

(1) The method only works at image magnifications which are high enough so that the resolution is determined by the probe size, and associated electron-solid interactions, rather than by the pixel size of the image. In practice this means magnifications in excess of about 20,000x for a 512*512 pixel image.

(2) A key assumption in this approach is that the specimen being examined contains a continuous and essentially uniform distribution of spatial frequencies from DC up to frequencies in excess of the maximum value represented by the resolution. If this is not the case then the measured 'resolution' limit is instead the inherent structural size limit for the specimen. When this technique is employed with transmission electron microscopes thin amorphous metallic films are used as the sample since these have been shown to contain spatial information to dimensions below 0.1nm. In the case of scanning electron microscopy, by

comparison, it is hard to find samples with spatial detail even approaching the nanometer scale. The Au-Pd layer on silicon shown in figure (1) and used for the analysis demonstrated in figure (3) has good equi-axed detail down to below 2nm, but all of the structures in the image are close to the same size scale which makes this sample of limited value for resolutions below 5nm. Postek and Vladar.⁷ have recently reported progress in fabricating special test samples with reproducible high frequency spectral detail from silicon but until such samples become widely available the technique must continue to be employed on samples where the true spatial spectrum of the specimen is unknown and is probably far less than ideal. As a result SEM resolutions determined in this manner are likely to be unduly pessimistic.

(3) The accuracy of the resolution determination depends on the accuracy with which the user can distinguish signal from noise. In fact on a pixel by pixel basis such a distinction is impossible from a single image. Since the signal to noise ratio falls towards unity at the resolution limit the boundary between signal information and noise is poorly defined and its exact position must be defined on the basis of arbitrary choices made by the user, for example by setting the boundary as occurring at some fixed fraction of the peak signal intensity, typically 10% corresponding to the Rayleigh criterion value, or relying on the skill of the user to make an appropriate choice. It is this problem which is discussed in the remainder of this paper.

4. CROSS CORRELATION

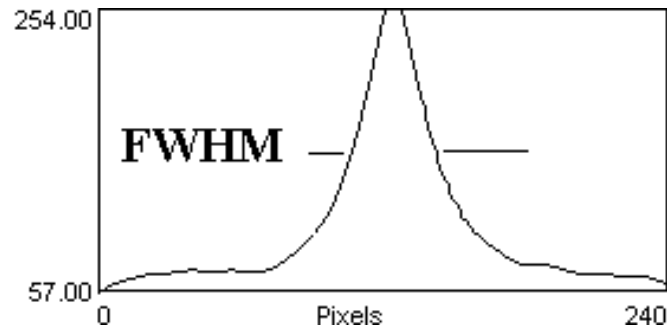
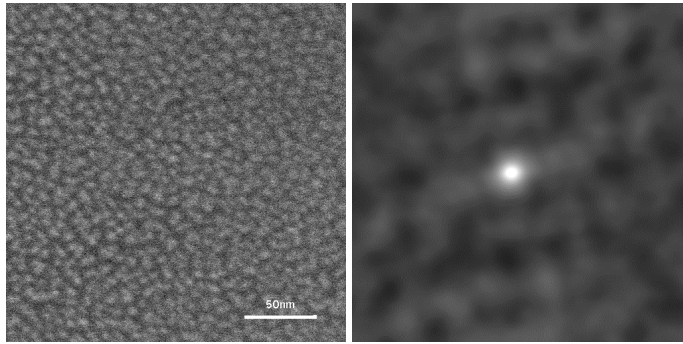
The use of the cross-correlation function^{8,9} provides a useful alternative to the straightforward Fourier analysis discussed above because it avoids the problem of distinguishing signal from noise. The cross-correlation function (CCF) can be written as

$$c(i, j) = \iint_{-\infty}^{\infty} C(u, v) e^{2\pi i(ux + vy)} du dv \quad (2)$$

where $C(u, v) = F(u, v) * G^*(u, v)$ and $F(u, v)$ and $G(u, v)$ are the two dimensional power spectra of images $f(x, y)$ and $g(x, y)$. If $f(x, y)$ and $g(x, y)$ are two samples of the same image separated by a few pixels then the CCF shows a sharp peak, offset from the center by an amount representing the pixel offset between the images, and with a full width at half maximum which corresponds to the Rayleigh criterion for the resolution of the image. This is equivalent to the statement that detail in the image will be correlated over a scale equal to the image resolution but noise is random pixel to pixel and so is uncorrelated.

The peak to background ratio of the CCF can also be used to provide an estimate of the signal to noise ratio of the image itself. Although the signal to noise ratio is not as useful a diagnostic of the imaging system as a measurement of the detector quantum efficiency (DQE) of the detectors¹⁰ if a standard sample is used then it provides a rapid way of monitoring the variation in performance as a function of time. Typical high resolution images so far analyzed show effective S/N ratios between 2 and 10, a figure which is significantly lower than the minimum value theoretically required by the Rose criterion for a statistically valid image¹¹. The fact that useful information can still be obtained from such images does not invalidate the Rose criterion because that is concerned with single pixels, whereas the brain can average and analyze detail spread over many pixels at one time.

As implemented in the SMART macro the user must first select a region of interest in the image. After the routine obtains the FFT of this region the program then selects a second area identical to the first in size but shifted in position by 10 to 20 pixels and obtains that FFT. Equation (2) is then used to compute the CCF, a line profile is taken through the CCF peak and the resolution and the image signal to noise ratio are reported from a measurement of the peak. Figure (4) demonstrates the application of this method to the Au-Pd test structure of figure (1). Figure 4(a) shows the chosen area (ROI) from the image, and figure 4(b) then shows the computed CCF plotted as a two dimensional image in which brightness is a measure of the value of $c(i, j)$ in equation (2). Figure 4(c) then shows the profile across the CCF peak. The full width half maximum (FWHM) of the peak is 36 pixels corresponding to a resolution of 4.2nm and the signal to noise ratio is seen to be just under 5:1



4. CCF analysis of a micrograph. (a) the analyzed ROI; (b) the cross correlation function plot; (c) the intensity plot across the CCF peak showing the definition of the resolution as the peak FWHM and the signal to noise.

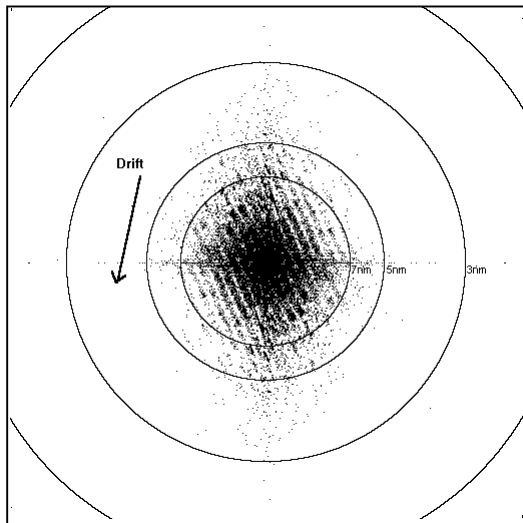
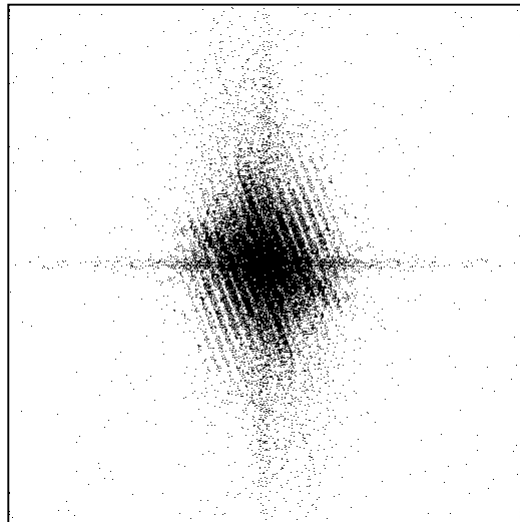
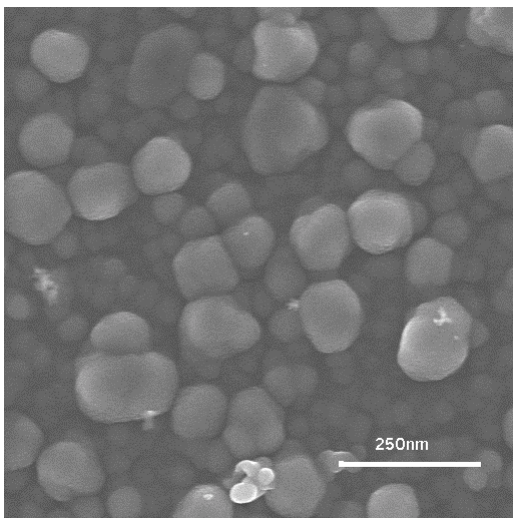
The advantage of the CCF method is that no decisions need to be made about what is 'signal' and what is 'noise' so the process can be carried out without operator intervention and is very rapid in execution. Although the resolution value from the CCF is currently only measured along one axis it would be simple to measure the resolution in other directions to estimate the astigmatism of the image. The CCF procedure is also not as sensitive to the exact nature of the specimen as the original power spectrum method and a wide range of spatial frequencies in the micrograph is not as critical an issue to the quality of the result. However, for successful application the CCF method requires a sample which is relatively homogeneous in character and is free from high contrast features in the field of view and this limits its utility under some conditions. Resolutions measured using the CCF method agree quite well with those obtained from the direct Fourier analysis method although they tend to be slightly more pessimistic because they do not confuse noise with signal.

One interesting application of this technique is the measurement of the physical probe size of an SEM. A simple scanning transmission electron microscopy (STEM) adapter installed in the SEM is used to observe a thin (<10nm) carbon film stretched across a transmission electron microscope (TEM) support grid. Because the film is thin the broadening of the beam in the film is negligible and so the resolution of the STEM image is equal to the probe diameter. A CCF analysis of the phase noise in the bright field STEM image of the carbon film directly yields the probe diameter of the SEM under these conditions. Because the contrast in such an image is low the standard FFT technique fails in this case.

5. TWO IMAGE ANALYSIS

The diffractograms of two superimposed but slightly shifted micrographs recorded sequentially from the same area can also be used to estimate the resolution in an image. The result, if the images are identical, is that the diffractogram produced by the superimposed image is equal to the diffractogram of a single image modulated by a periodic function which is the diffractogram of two point sources separated by the same amount as the images were shifted. This procedure, first suggested by Frank et al.¹² has been widely used for testing the resolution of transmission electron microscopes but has also been applied to the study of SEM performance¹³. The method has two key advantages; first this method distinguishes between detail and random noise because the true image information detail will be present in both copies of micrograph whereas random noise, although present in both cases, is not correlated between them. Hence portions of the diffractogram corresponding to image information are modulated by the periodic envelope while noise is left unmodulated. Determining the boundary between signal and noise is therefore much easier. In fact it can be shown that coherent detail in the combination diffractogram is enhanced by a factor of four compared to incoherent noise which represents a significant factor. Second, because two sequential images are used an analysis of the diffractogram provides additional information about the stability and behavior of the SEM as a function of time.

Figure (5) shows the procedure for this type of analysis using the SMART macro. The user loads two images of the same area of the same sample recorded sequentially. The first of such a pair of images is shown in figure 5(a). A region of interest is selected on the first image by the user. The program copies this ROI, then go to the second member of the image pair and copies an ROI from that. This second ROI is identical in size to the first but is shifted laterally by 16 pixels. (The amount of the shift is not critical but should typically be a few percent of the width of the ROI). The FFT is then computed producing a diffractogram of the type shown in figure 5(b). The fringes modulating the signal information are now evident and the boundary between signal information and noise is clearly visible. (Note that if the fringes extend to the edges of the diffractogram then the image resolution is pixel limited rather than spot size limited). The program then superimposes a calibrated scale on the diffractogram (figure 5c) enabling the resolution to be determined directly, while the level of astigmatism can be judged visually. Resolution values measured in this manner tend to be slightly worse than those obtained from a single image as would be expected from the fact that it is the performance over some relatively long period of time that is now being evaluated,



5. Analysis of sequential image pairs. (a) 512*512 pixel ROI of one of the image pair (Secondary electron image recorded from oxide on silicon); (b) the two dimensional power spectrum (diffractogram) of the composite image formed as described in the text. Note that the fringes do not extend into the random noise and so delineate the information bearing region of the transform. (c) The diffractogram with the superimposed calibration scale showing an image resolution of about 8nm. The image offset was horizontal but the fringes are seen to be rotated by about 25 degrees. The drift vector which has caused this rotation is shown.

Since the composite image used in this analysis was produced by the addition of two ROIs shifted laterally by a certain number of pixels it would be expected that the fringes would be vertical (i.e. normal to the line joining the two point sources). If however any shift in the image occurs between the first and second exposures, due to stage drift, beam instability, or sample charging, then the fringes will reflect this change

in relative image orientation. If the angle of rotation of the fringes with respect to the vertical is θ then D, the magnitude of the drift between the two exposures, is given as

$$D = 2 \cdot \text{offset} \cdot \sin(\theta/2) \quad (3)$$

where the offset is the pixel size multiplied by the number of pixels offset between the exposures. Here the offset is 16 pixels, the pixel size is 0.9nm/pixel, and $\theta = 25$ degrees so the drift $D = 6.4$ nm over a period of 40 seconds.

6. CONCLUSIONS

Fourier based techniques for the analysis of SEM imaging performance are a significant improvement over the anecdotal method based on visual inspection of an image. Reliable data on imaging resolution and probe size can be obtained, together with data on related properties of the instrument such as the signal to noise ratio and the stability. These measurements can be made in an automated fashion and so are suitable for use on machines that run in unattended mode. Taken together the parameters that are reported provide the basic information needed to begin to characterize the major aspects of instrument behavior.

ACKNOWLEDGEMENTS

The authors are grateful to Drs. M Postek, A Vladar, M Davidson, and E Voelkl for valuable discussions. This work was partially funded by the Semiconductor Research Corporation under contract 96-LJ-413. The contract monitor is Dr.D.Herr. Oak Ridge National Laboratory is operated by Lockheed Martin Energy Research Corporation for the U.S. Department of Energy under contract number DE-AC05-96OR22464.

REFERENCES

1. 1999 International Technology Roadmap for Semiconductors, Semiconductor Industry Association.
2. T A Dodson and D C Joy, (1990), 'Resolution measurement of SEM images', Proc. 12th Int. Conf. on Electron Microscopy, 406-7
3. NIH Image can be downloaded from <http://rsb.info.nih.nih-image>
4. SCION Image is an authorized port of the Macintosh NIH Image program to Window 95 and 98 platforms. It can be downloaded from www.scioncorp.com
5. 'Metrologia' from SPECTEL Research Inc. See also A E Vladar, M T Postek, M P Davidson (1997), 'Image Sharpness Measurement in Scanning Electron Microscopy -II', SCANNING **20**, 24-34
6. SMART can be downloaded from <http://web.utk.edu/~srcutk>.
7. M Postek and A Vladar (1999) personal communication.
8. J.Frank (1980), in *Computer Processing of Electron Microscope Images*, (Springer-Verlag:NY), p187-222.
9. H K Youn and R F Egerton, (1997), Proc. Microscopical Society of Canada, 'Resolution measurement of SEM using CCF', **24**, 63-64
10. D C Joy, C S Joy, and R D Bunn, (1996), 'Measurement of detector efficiencies in the SEM', SCANNING **18**, 533-538
11. J I Goldstein, D E Newbury, P Echlin, D C Joy, E Lifshin, C E Fiori,, 'Practical Scanning Electron Microscopy and Microanalysis', Plenum Publishing, New York, 1992
12. J Frank, P Bussler, R Langer, W Hoppe (1970), 'Transmission electron diffractograms' (in German), Ber. Busenges. Phys.Chem., **74**, 1105-1115
13. S J Erasmus, D M Holburn, K C A Smith (1980), 'On-line computation of diffractograms for the analysis of SEM images', Inst. Phys. Conf. Ser. **52**, 73-76